

Strength evaluation of concrete-filled steel tubes subjected to axial-flexural loading by ACI and AISC-LRFD codes along with three dimensional nonlinear analysis

S. B. Beheshti-Aval*

Received: February 2011, Revised: January 2012, Accepted: June 2012

Abstract

A comparison between design codes i.e. ACI and AISC-LRFD in evaluation of flexural strength of concrete filled steel tubular columns (CFTs) is examined. For this purpose an analytical study on the response of CFTs under axial-flexural loading is carried using three-dimensional finite elements with elasto-plastic model for concrete with cracking and crushing capability and elasto-plastic kinematic hardening model for steel. The accuracy of the model is verified against previous test results. The nonlinear modeling of CFT columns shows that the minimum thickness that recommended by ACI and AISC-LRFD to prevent local buckling before the steel shell yielding for CFT columns could be decreased. The comparison of analytical results and codes indicates that the accuracy of ACI method in estimation of axial-flexural strength of CFT columns is more appropriate than AISC-LRFD. The ACI lateral strength of CFTs is located on upper bond of the AISC-LRFD's provisions. AISC-LRFD estimates the lateral strength conservatively but ACI in some ranges such as in short columns or under high axial load levels computes lateral strength in non-conservative manner. Supplementary provisions for post local buckling strength of CFT columns should be incorporated in high seismic region. This effect would be pronounced for column with high aspect ratio and short columns.

Keywords: Code; Concrete; Steel; Finite element modeling; Composite member; Confinement.

1. Introduction

The use of concrete-filled steel tubular columns (CFTs) in structural frames has increased in United States, Japan, China and Australia during the past the past two decades. They have been used as columns or bracings in high-rise buildings, piers for bridges, and so on. CFT combines potential benefits of steel and concrete to provide a superior structural system, particularly for seismic applications. The tube increases the strength and ductility of concrete through confinement, while concrete in return prevents the inward buckling of the tube. Additional benefits are realized through speed of construction, use of standard connections, and eliminating the need for a separate concrete form. Because of high seismic performance of this type of elements, their use becomes more and more popular in recent years. Utilizing of precise analytical calculation demanded cumbersome nonlinear three dimensional modeling of this type of infrastructures. So designers prefer to adopt closed form

formulation based on codes. In response to these demands, the ultimate strength of CFT column is incorporated several codes such as ACI Building Code (ACI 318-08) [1], Specification for Structural Steel Buildings (ANSI/AISC 360-05) [2], EC 4 [3], AS-5100, and CSA S16-01 [4], CECS-28:90 [5], AIJ [6]. Although codes encompass provisions for strength evaluation under a design procedure, their applicability are confined by limited range of design parameters. The applicability of codes provision in outside range of these parameters is questionable and main goal of this paper is answer to this doubt.

Design professionals who are familiar with ACI Building Code and AISC-LRFD Load and Resistance Factor Design practically used those codes to calculate CFT's strength under design loads. The superior of each choice for adopting of codes in designing of CFT columns under general loading is a great question for each designer. ACI views CFT is a concrete column that surrounded with steel tube. In contrast AISC-LRFD consider this column as a steel column that filled with concrete.

Since the behavior of CFT columns is mostly affected by the width-to-thickness D/t ratio, slenderness L/D ratio, and axial load N/N_o level, in this paper the accuracy of codes is compared with detailed analytical method.

* Corresponding Author: beheshti@kntu.ac.ir
Associate Professor, Civil Engineering Faculty, K.N.Toosi University
of Technology, Tehran, Iran

2. Previous research

With a literature survey, one can find a comprehensive study has been done by a number of investigators in recent years. Research conducted on seismic behavior of CFT may be divided into experimental and analytical studies. Compared to analytical studies, more experimental work has been done on CFT. We can categorize these researches in two parts i.e. research that focused on axial strength and flexural strength. Refer to behavior of these columns under axial loads, we can find the extensive works [7-13]. Several other researchers focused their studies on flexural behavior of CFT columns [14-22]. Much of the analytical studies have been focused on computing the ultimate axial and flexural capacity of CFT members [23-28]. Nonlinear 3-D finite element analysis of CFT is rare in the analytical literature [22, 29]. They used this type of analysis in an individual rectangular or circular CFT stub or long box column subjected only axial or along flexural loading. Uses of frame elements were appeared in the several research works [e.g., 30-34].

Comparison between ACI and AISC-LRFD has been found in a few research works. Lundberg [35] gathered available experimental data for axially and laterally loaded CFT column on CFTs. In this study the calculating code based method of AISC-LRFD was compared with ultimate strength of experiments. The average strength of the axially loaded columns was about 1.32 times than AISC-LRFD predicted. It was concluded that current AISC-LRFD specification was not addressed composite action of CFTs subjected axial loads. Schneider [36] tested 14 specimens with circular, square and rectangular section under concentric axial loads. D/t ratios in this study were ranged from 17 to 50 and L/D , from 4.0 to 4.8. The shape of the steel tube and the aspect ratio were the primary parameters in the test program. He concluded that for small dimensional CFT columns, smaller D/t ratios provide a significant increase in yield load compared to the computed AISC-LRFD Specifications. In almost all cases the AISC-LRFD Specification provides a reasonable and conservative estimate for the axial strength of the CFT columns. In a few cases that the AISC-LRFD predicted load underestimated, the predicted yield load was no conservative by only 5% (two specimens). The average augmented strength in respect to AISC-LRFD Specification was 1.07. Zhang, and Shahrooz [37] assembled a wide range of experimental data to examine the success of two design codes (i.e. ACI and AISC-LRFD) in calculating the axial strength of CFT columns. The adequacy of codes also examined under out-ranged strength of steel and concrete, permitted by codes. They found strength computed by ACI and AISC-LRFD Specification can vary significantly. Neither two codes are applicable for cases in which high-strength steel tubes are used. And finally they suggested correction to the ACI method for CFT column in which the steel tube is assumed to have fully yielded.

Recently Lue et al. [38] inspected the applicability of AISC-LRFD to predict the axial strength of CFT columns with high-strength concrete. This study aimed to assess if the LRFD CFT column formulas were applicable to intermediate to long rectangular columns with higher concrete strengths (varying between 29 and 84 MPa). Various formulas and relevant

provisions for CFT columns as specified in the major design codes including AISC-LRFD [2], EC4 [3], AS-5100 [39], and CSA S16-01[4] were examined and compared. The design CFT strength predicted by the AISC-LRFD formulas and the test results were found to be in good agreement. The higher concrete strengths limiting value of 70 MPa proposed in the AISC-LRFD appears acceptable.

In the previous studies the accuracy of codes in each range of effective parameters on behavior of CFT columns were not studied. The success of codes in predicting of capacity of CFT column under general loading in a wide range of parameters is unknown. Due to use of out ranged-parameter CFT columns in several buildings, applicability of design codes for design purposes seems necessary.

3. Flexural strength of cft columns

3.1. Analytical method

Since the particular effect of some major aspects of CFT such as local buckling, bond deterioration, slippages and interface friction, and variation of confinement during loading between steel shell and concrete core can not directly considered in a frame element analysis, So for the study of behavior of CFT, three-dimensional modeling is obligatory.

Among the available FE programs, ANSYS® [40] is chosen owing to its comprehensive element library and material models that are suitable for the analysis of CFT. Fig. 1 shows typical FE meshes for circular and square CFT columns. Due to symmetry and loading conditions, only a half section of the column section is modeled. Concrete is modeled using eight-noded *SOLID65* elements with three degrees of freedom at each node. The element is capable of simulating smeared cracking in three orthogonal directions, crushing and plastic deformations. Plasticity is controlled before cracking or crushing is checked. Cracking initiates if any of the principal stresses exceeds the tensile strength of concrete. The presence of a crack at an integration point is represented through modification of the stress-strain relations by introducing a plane of weakness in the direction normal to the crack face. A shear strength reduction factor is considered for subsequent loads, which induce sliding across the crack face. If the crack closes, all compressive stresses normal to the crack plane are then transmitted across the crack, and the shear transfer coefficient for a closed crack is introduced.

Crushing occurs when all principal stresses are compressive, and the multi-axial state of stress reaches the five-parameter failure surface defined by Willam and Warnke [41]. The 3D-view of this failure surface in space of principal stresses is shown in Fig.2a. If crushing occurs at an integration point, the material strength is assumed to have fully degraded to the extent that its contribution to the element stiffness could be ignored. Creep and shrinkage of concrete are both ignored, since they have been found to have negligible influence on CFT [42].

Steel tube is modeled using four-noded SHELL43 element with six degrees of freedom at each node. Capabilities of the element include plasticity with strain hardening, stress stiffening, large deformations and large strains. The kinematic hardening option for steel plasticity properly models the Baushinger effect under cyclic loads. The stress-strain

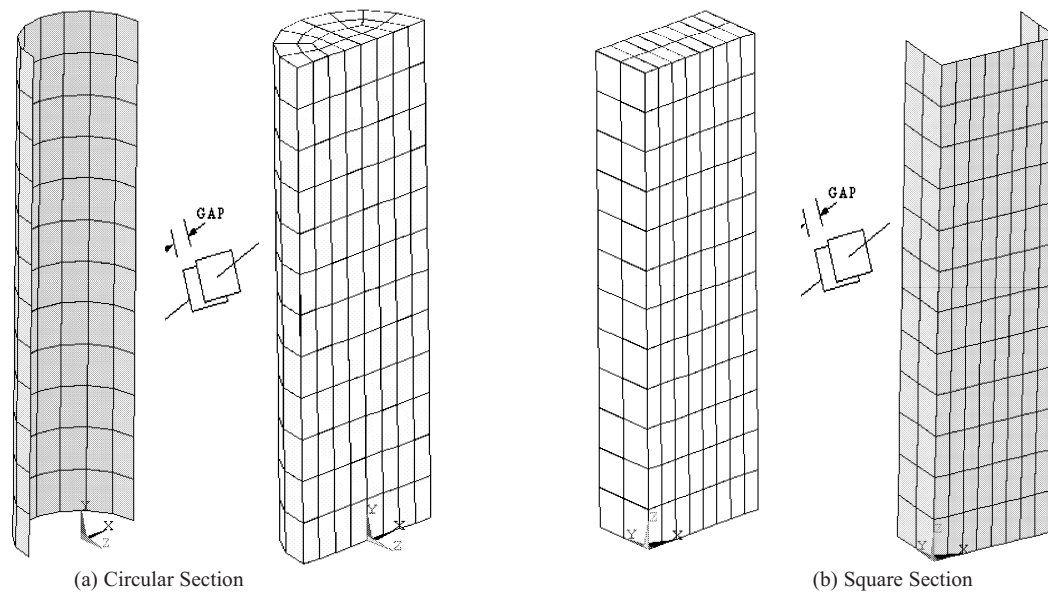


Fig. 1. Typical Finite Element Mesh

behavior and the translation of the yield surface in deviatoric stress space are shown in Fig. 2b. The effects of residual stresses in the tube are neglected, mainly because recent studies have suggested their insignificant influence on the behavior of CFT [22].

The concrete-steel interface is modeled using CONTACT52 gap elements, placed between the adjacent nodes of steel tube and concrete core. The gap elements have a fixed contact direction perpendicular to the tube surface. The concrete core and steel tube are assumed to be initially in contact with each other, i.e., with zero initial separation or gap. The element can maintain or break physical contact between concrete and steel. It supports only compression in the normal direction and shear in the two tangential directions. A coefficient of friction of 0.3 is used in all parametric studies for the slippage or sliding between steel tube and concrete core.

The equilibrium equations are solved using an adaptive descent method [43]. The method switches to a stiffer matrix, if convergence difficulties are encountered; and to the full tangent stiffness as the solution converges. The nonlinear solution is quite sensitive to the number of sub-steps in each load step. This is due to some negative pivots that may have

been associated with a non-localized materially-unstable equilibrium path. There is some softening in the description of the tensile stress-strain relation in the concrete model. Therefore, the response may show some local minima or maxima [44]. Due to the softening behavior of concrete, a displacement control strategy is adopted.

Conventional buckling analysis of the tube is carried out using large deformation analysis in two steps: (1) buckling modes and buckling loads are estimated through eigen-value analysis, and (2) load-displacement analysis is carried out using the imperfections suggested by the eigen modes. While expansion of concrete core provides the necessary imperfections for buckling of the tube under axial loads, transverse deflections of beam-columns provides the additional eccentricity needed for the buckling. The onset of buckling is marked by a non positive-definite total stiffness matrix, which is the result of high compressive membrane stresses in the tube during the loading history. The method of stress stiffening is utilized in the solution strategy. The method considers stiffening of a structure due to its stress state. This stiffening effect couples the in-plane and transverse displacements. It is normally considered for thin structures, such as steel tube in CFT columns, with very small

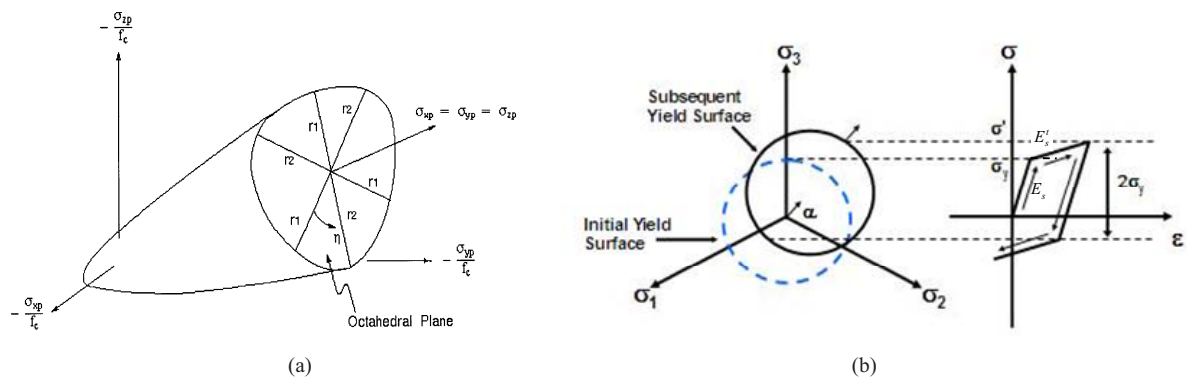


Fig. 2. The material behaviors a) The 3D-view of the failure surface for concrete. b) The stress-strain behavior and the yield surface in deviatoric stress space

bending stiffness as compared to the axial stiffness. With large deformations, the stress stiffness matrix forms part of the tangent matrix, thus affecting the rate of convergence but not the final converged solution.

Local instability or buckling in the steel tube is the major cause of strength degradation in CFT columns with high width-to-thickness D/t ratio. Concrete core helps prevent inward buckling of the tube. The initiation of local buckling can be traced by examining the normal contact force between the tube and concrete core. While confining pressure continues to increase in the un-buckled regions, confinement vanishes at the location of local buckling. Since gap elements can not take any tensile stresses, the release of contact forces indicates outward buckling of the tube. The local buckling phenomenon can often be observed near column ends under shear loads. The large shear stress at the steel-concrete interface near the supports causes separation of the tube from concrete, eventually leading to its local buckling.

4. Current ACI and AISC-LRFD method

Each of these codes does not consider the enhanced performance of CFT columns owing to almost complete confinement of the concrete core. The ACI design requirements for composite columns are similar to those for conventionally reinforced concrete column design, with modifications of certain parameters. These parameters are effective radius of gyration and flexural stiffness (Equation 1 and 2).

$$r = \sqrt{[(E_c I_c / 5) + E_s I_s] / [(E_c A_c / 5) + E_s A_s]} \quad (1)$$

$$EI = (E_c I_c / 5) / (1 + \beta_d) + E_s I_s \quad (2)$$

Where E_c and E_s = elastic modulus of concrete and I_s steel respectively; I_c and I_s = moment of inertia of section for concrete and steel respectively; A_c and A_s = area of concrete and steel section respectively β_d = the ratio of the maximum factored axial sustained load to the maximum factored axial load. According to the code commentary, the radius of gyration is modified because the rules allowed for estimating the radius of gyration for ordinary reinforced concrete columns are overallly conservative for CFTs. The commentary also indicates to account for creep effects. The ACI evaluates ultimate axial strength of CFTs as follow:

$$P_0 = A_s f_y + 0.85 A_c f'_c \quad (3)$$

f_y and f'_c are yield strength and specified compressive strength of concrete core. Code recommends using the similar

equations as R.C. Fig. 3 shows the stress and strain distribution in CFT 's section according to ACI.

For prevention of local buckling before yielding, both of the ACI and AISC-LRFD suggest the minimum thickness for square and circular sections as follow:

$$t_{\min} = 0.58b \sqrt{\frac{f_y}{E}} \text{ (ACI)} , \quad t_{\min} = 0.44b \sqrt{\frac{f_y}{E}} \text{ (AISC-LRFD)}$$

: Square Sections (4a)

$$t_{\min} = 0.35D \sqrt{\frac{f_y}{E}} \text{ (ACI)} , \quad t_{\min} = 6.67D \frac{f_y}{E} \text{ (AISC-LRFD)}$$

: Circular Sections (4b)

Where b and D are overall width of rectangular and circular CFT section, respectively. The aforementioned amounts are the same values that are provided for hollow steel sections.

Likewise, the AISC-LRFD code considers CFT column design to be similar to steel column design, again with modifications to the steel yield strength, modulus of elasticity, and radius of gyration to account for effect of the concrete. The AISC-LRFD Specification does not provide detailed requirements for reinforcing bar spacing, splices, and so on. Thereby it is likely logical that the requirement in this regard of the ACI Code should be followed for situation not clearly covered by the AISC-LRFD Specification. Code places minimum limitation on the percentage area of steel (1 percent of the total composite cross section) to qualify for design as a steel member. If this requirement was not fulfilled, CFT column should be considered as a concrete column and designed based on ACI code. The concrete strength should be casted in range of 21 to 70 MPa. This limitation is owing to nonexistence of enough experimental data for the higher strength concrete. The lower range is pertaining to accessibility of high performance and adequate durability of concrete. In this code no provision is found for minimum cement grade. Based on relationships (4), minimum thicknesses of the shell have the lower values as per AISC-LRFD in comparison with ACI. The steel stress yielding is confined by 525 MPa and additional strength is ignored in this code. In AISC-LRFD, the nominal strength is evaluated according to ultimate loading. Then reduction factors are applied. The ultimate stress distribution, which is assumed in analysis, is shown in Fig. 4. Two methods in the AISC-LRFD are provided for determining the nominal strength of composite sections: the plastic stress distribution method and the strain-compatibility method. The latter method is alike to ACI approach to predict strength of RC sections. As noted in

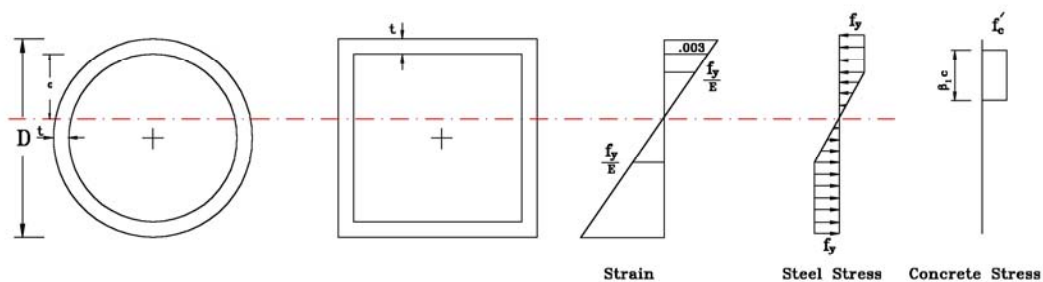


Fig. 3. The stress and strain distribution in CFT's sections according to ACI

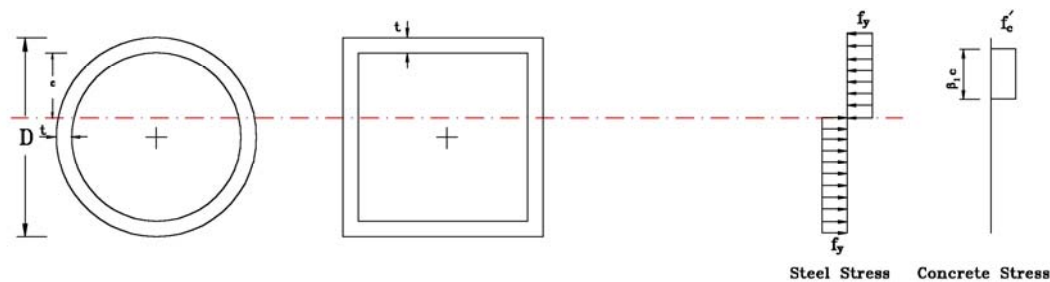


Fig. 4. The stress and strain distribution in CFT's sections according to AISC-LRFD

spec, the strain compatibility method restricted to determine nominal strength for irregular sections and for cases where the steel does not exhibit elasto-plastic behavior. The design strength is:

$$P_u = 0.75P_n \quad (5)$$

For axially-loaded CFT columns shall be determined for the limit state of flexural buckling based on column slenderness:

$$\text{Where } P_e \geq 0.44P_0: \quad P_n = P_0 \left[0.658 \left(\frac{P_0}{P_e} \right) \right] \quad (6a)$$

$$\text{Where } P_e < 0.44P_0: \quad P_n = 0.877P_e \quad (6b)$$

Where $P_0 = A_s f_y + C_2 A_c f'_c$ ($C_2 = 0.85$ for rectangular sections and 0.95 for circular sections), and:

$$P_0 = \pi^2 (EI_{eff}) / (kL)^2 \quad (7)$$

The modified elastic modulus and modified yield stress of CFT column are defined based on following relations:

$$EI_{eff} = E_s I_s + C_3 E_c I_c, \quad C_3 = 0.6 + 2 \left(\frac{A_c}{A_c + A_s} \right) \leq 0.9 \quad (8)$$

No provision are given in either codes for CFT design of high seismicity regions.

5. Verification of analytical model

The accuracy of the FE model is verified against test results of 4 beam-column specimens of Sakino and Ishibashi [15] with fixed supports at both ends. After the specimen is loaded axially to a preset level, the axial load is maintained and a prescribed lateral displacement history is applied at the top. The geometric and material properties and axial loads for tested specimens are summarized in Table 1, where N is

applied axial load, N_o (i.e., P_o) is column capacity, as calculated by the ACI, D is outer width or height of the square tube section, t is tube thickness, L is column length.

Fig. 5 compares predicted load-displacement curves with monotonic test results for the 4 test specimens. The stress-strain relation for the steel tube was considered as bilinear with a strain hardening slope at 1% of the initial elastic modulus of steel. Lateral displacements are normalized as percent drift R with respect to the column height. Favorable agreement is generally noted for the analytical predictions. Slight discrepancies may be attributed to the material models that are available in ANSYS®. The local maxima/minima and snap-trough or snap-back are attributed to cracking and crushing of concrete, local buckling of steel tube, and sudden variation of stiffness of gap elements, as previously identified by Crisfield [45]. The general slope of the post-peak descending branch depends on the mesh size [46].

6. Sensitivity study of codes to effective parameters on CFT

Analytical studies and experiments have confirmed that behavior of CFT columns is mostly affected by the width-to-thickness D/t ratio, slenderness L/D ratio, and axial load N/N_o level. The accuracy of Codes in evaluation of flexural strength is compared with analytical method in the following sections:

6.1. Aspect ratio considerations

Table 2 shows the geometric and material properties and axial loads for the case study. The comparison between flexural strength provisions by codes with analytical value versus change of aspect ratio was carried out with 8 columns, half of which with a square section (SC), and the other half with a circular section (CC). The same loading pattern was used as that of the verification test specimens. Four D/t ratios of 25, 50, 75, and 100 were considered by varying the tube

Table 1. Geometric and material properties and axial loads for verification specimens [10]

Specimen No.	N (kN)	N/N_o	D (mm)	t (mm)	L (mm)	L/D	D/t	f'_c (MPa)	f_y (MPa)
SI85-I	140	0.19	100	4.25	300	3.0	24	22.5	322
SI85-II	89	0.18	100	2.20	300	3.0	45	20.9	297
SI85-III	158	0.28	100	3.98	300	3.0	34	22.5	322
SI85-IV	130	0.46	100	2.20	300	3.0	45	20.9	384

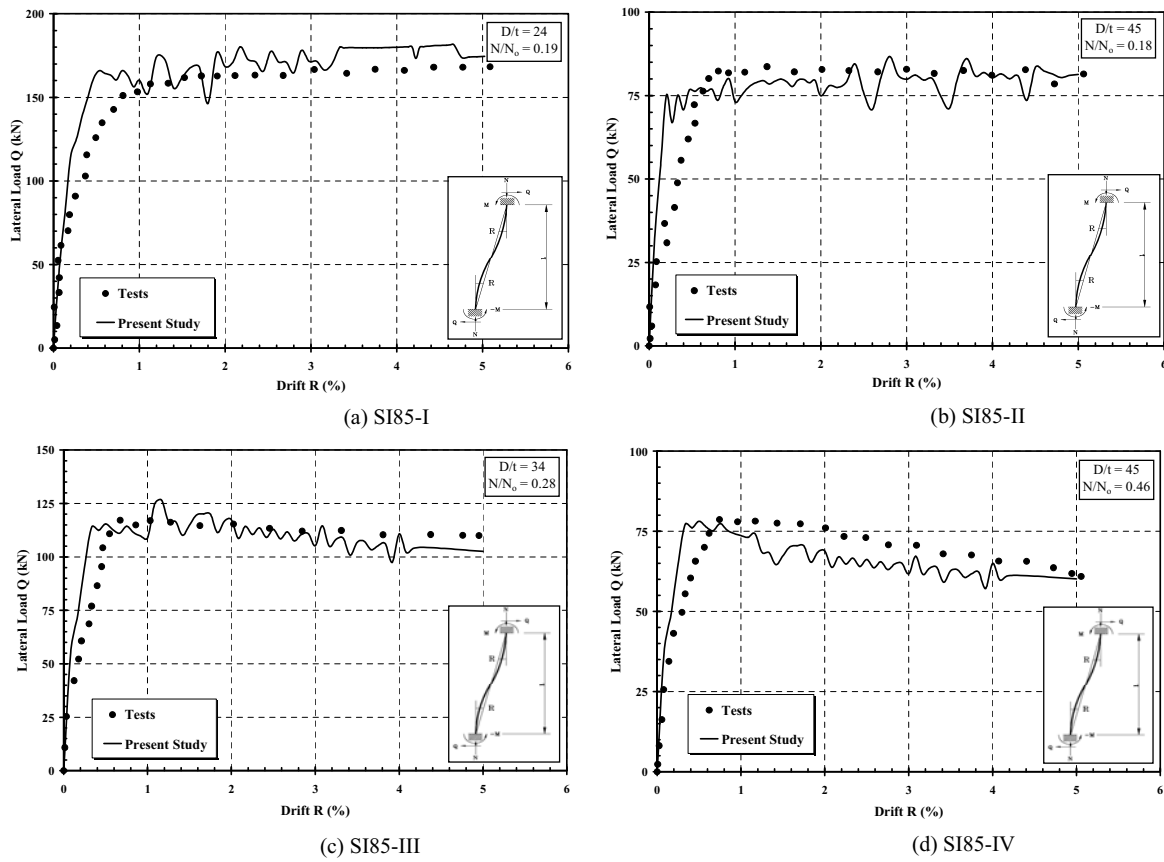


Fig. 5. Comparison of analytical and experimental results

thickness. All columns had the same L/D ratio of 4, and were all tested at the same axial load level of 20%. The compressive strength of concrete core and the yield stress of steel tube were 22.5 MPa and 240 MPa, respectively. The stress-strain relation for the tube was considered as bilinear with a strain hardening slope (E'_s) at 1% of the initial elastic modulus of steel (E_s).

Based on relations (4) the minimum thickness of steel shell based its properties in Table 2 are calculated as:

$$t_{min} = 6.0 \text{ mm (ACI)}, 4.6 \text{ mm (AISC)} \quad : \text{ Square Sections}$$

$$t_{min} = 3.6 \text{ mm (ACI)}, 2.4 \text{ mm (AISC)} \quad : \text{ Circular Sections}$$

The maximum lateral strength of CFT and the corresponding

hollow steel columns (HSC depicted at Table 2) are evaluated with analytical model and code's provisions vs. D/t ratio are shown in Fig. 6. The Fig.7 shows the ratios of code values to values predicted by present study for changing aspect ratio. Some conclusions can be expected as:

i. According to table. 2 the columns SC-DC-I, SC-DC-II, and CC-DC-I hold a steel-shell's thickness less than the minimum values permitted by codes. One can find the analytical values located upper bond of code's predictions for CFT column. For two square CFT sections (SC-DC-I, SC-DC-II), the analytical values is greater than code provisions, but the analytical results of hollow SC-DC-I section has lower strength than AISC-LRFD. The later comparison is reasonable, because the assumption of no buckling is

Table 2. Properties of specimens for the width-to-thickness ratio case study

Specimen No.	Section	N (kN)	N/N_0	D (mm)	t (mm)	L (mm)	L/D	D/t	f'_c (MPa)	f_y (MPa)	E'_s/E_s
SC-DT-I	Square	426	0.20	300	3	1200	4	100	22.5	240	0.01
SC-DT-II		470	0.20	300	4	1200	4	75	22.5	240	0.01
SC-DT-III		557	0.20	300	6	1200	4	50	22.5	240	0.01
SC-DT-IV		811	0.20	300	12	1200	4	25	22.5	240	0.01
CC-DT-I	Circle	335	0.20	300	3	1200	4	100	22.5	240	0.01
CC-DT-II		369	0.20	300	4	1200	4	75	22.5	240	0.01
CC-DT-III		444	0.20	300	6	1200	4	50	22.5	240	0.01
CC-DT-IV		637	0.20	300	12	1200	4	25	22.5	240	0.01

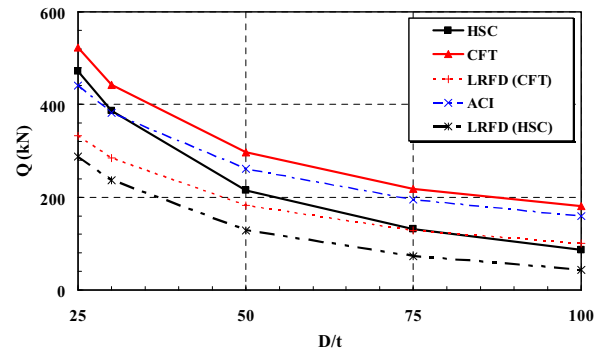
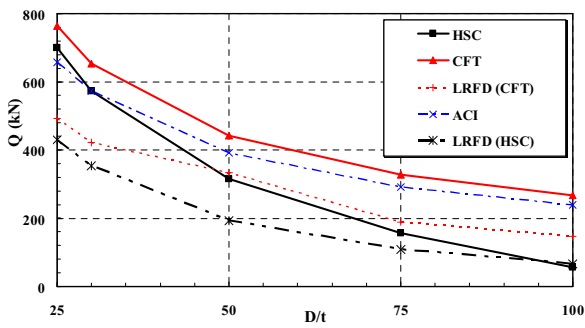


Fig. 6. The lateral strength of columns vs. aspect ratio

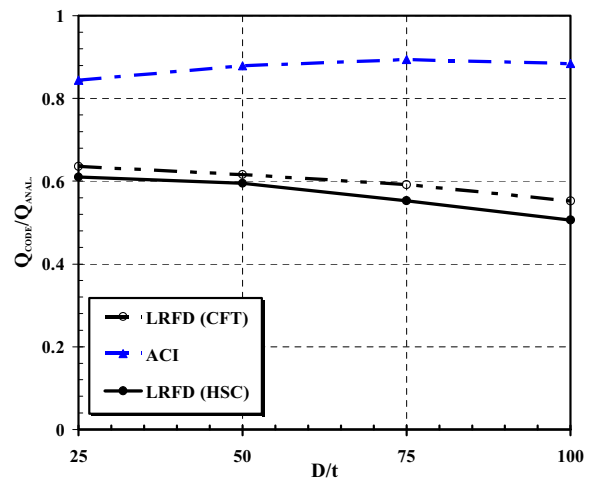
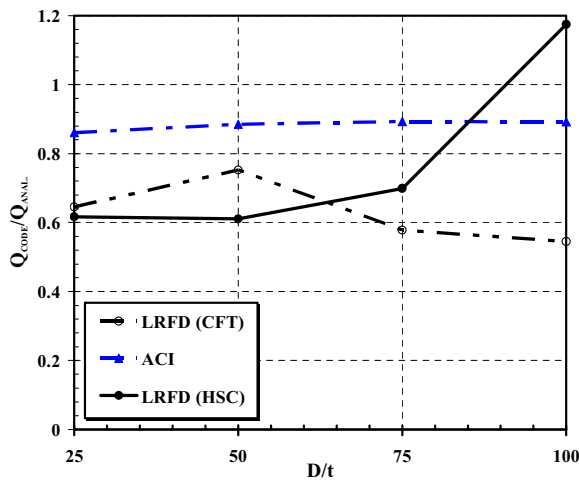


Fig. 7. The comparison between codes and present study for changing aspect ratio

presumed in AISC-LRFD equations. But for CFT sections with high aspect ratio, it is reasonable to modify the equation (4) to less value. It is seemed for hollow circular sections the equation that suggested for AISC-LRFD for minimum thickness should be modified to less value. This equations that is formulated for hollow steel columns, are conservative for CFT columns

ii. ACI shows greater shear strength than AISC-LRFD for CFT column, the close estimation of lateral strength is observed for ACI results. Thereby AISC-LRFD estimates lateral strength of CFTs more conservative than ACI

iii. Two codes provide close estimation of shear strength in moderate aspect ratio ($D/t=50$).

iv. The concrete and steel strength in code's expressions should be modified for level of confinement based on change of D/t index.

v. For CFT square sections with low aspect ratio, ACI shows good estimation of post-peak strength.

vi. Due to ignoring local buckling, AISC-LRFD shows greater value to analytical results in large aspect ratio for hollow steel columns (HSC).

vii. For moderate level of axial loads and slenderness, codes are safe in evaluation of lateral strength if CFTs column ($N/N_0=0.2$ and $L/D=4$).

6.2. Slenderness index considerations

Table 3 shows the geometric and material properties and axial loads for the slenderness ratio case study. The comparisons with codes was carried out with 8 columns, half of which with a square section, and the other half with a circular section. The same loading pattern was used as that of the verification test specimens. Four L/D ratios of 2, 4, 6, and 8 were considered by varying the column length. All columns had the same D/t ratio of 50, and were all tested at the same axial load level of 20%. The compressive strength of concrete core and the yield stress of steel tube were 22.5 MPa and 240 MPa, respectively. The stress-strain relation for the steel tube was considered as bilinear with a strain hardening slope at 1% of the initial elastic modulus of steel.

The maximum lateral strength of CFT columns (depicted at Table 3) are evaluated with analytical model and code's provisions that are depicted in Fig. 8 vs. L/D ratio (slender index). The Fig. 9 shows the ratios of code values to values predicted by present study for changing slenderness ratio. Some conclusions can be expressed by comparison of following curves:

i. For wide range of changing slenderness, the lateral strength of ACI is greater than AISC-LRFD.

Table 3. Properties of specimens for the slenderness ratio case study

Specimen No.	Section	N (kN)	N/N_0	D (mm)	t (mm)	L (mm)	L/D	D/t	f'_c (MPa)	f_y (MPa)	E_s'/E_s
SC-LD-I	Square	470	0.20	300	4	600	2	50	22.5	240	0.01
SC-LD-II		470	0.20	300	4	1200	4	50	22.5	240	0.01
SC-D-III		470	0.20	300	4	1800	6	50	22.5	240	0.01
SC-LD-IV		470	0.20	300	4	2400	8	50	22.5	240	0.01
CC-LD-I	Circle	369	0.20	300	4	600	2	50	22.5	240	0.01
CC-LD-II		369	0.20	300	4	1200	4	50	22.5	240	0.01
CC-LD-III		369	0.20	300	4	1800	6	50	22.5	240	0.01
CC-LD-IV		369	0.20	300	4	2400	8	50	22.5	240	0.01

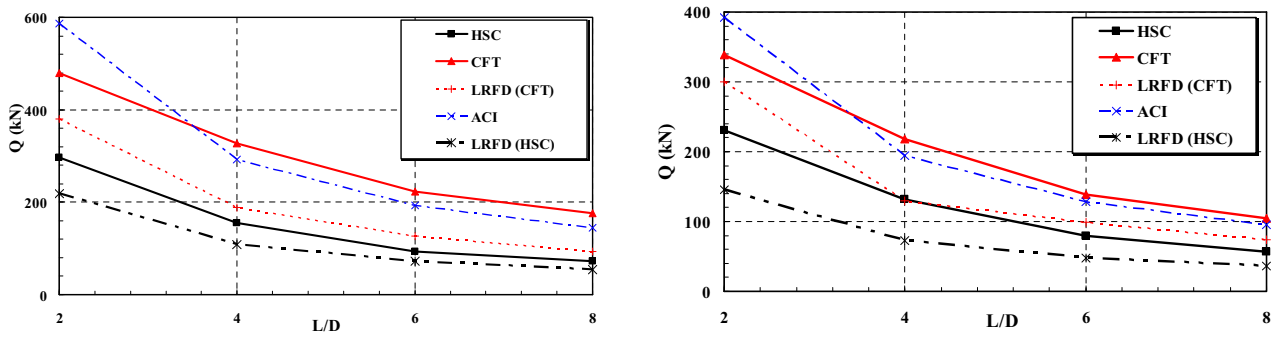


Fig. 8. The lateral strength of columns vs. slenderness ratio

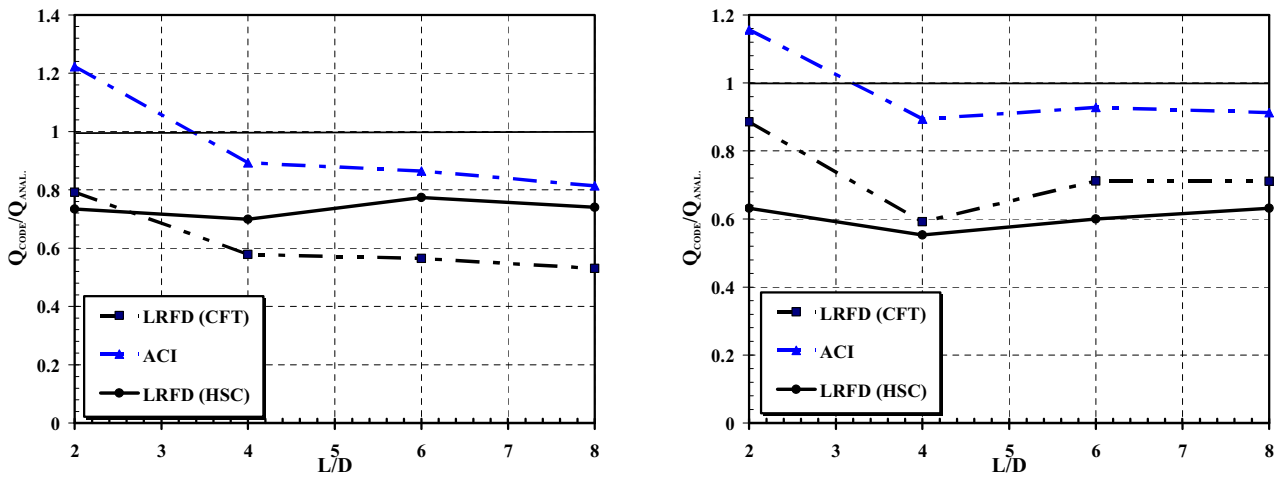


Fig. 9. The comparison between codes and present study for changing slenderness

ii. ACI values for short columns ($L/D=2$) are not conservative. In contrast AISC-LRFD computes the lateral strength for all applicable slenderness in conservative manner. Because the short column experience excessive local buckling (for low to moderate D/t) that it is not considered in ACI's equations. Also effects of shear deformation are not reflected for short column on codes equations.

iii. The deviation curves for CFTs in Fig. 9a, 9b are parallel. It shows in estimating of strength, two codes consider the

effect of slenderness in same manner. The steep slip is located in low slenderness range that indicates the effect of local buckling should be entered in this range.

iv. For square columns the effect of slenderness on accuracy of strength's estimation for hollow and CFT columns are in opposite manner i.e. for hollow section, AISC-LRFD is far away from analytical values during reducing of slenderness. But for CFT columns, these two values are in neighborhood.

6.3. Load level consideration

Table 4 shows the geometric and material properties and axial loads for the axial load level case study. The study was carried out with eight columns, half of which with a square section, and the other half with a circular section. The same loading pattern was used as that of the verification test specimens. Four different N/N_0 ratios of 0, 20%, 35%, and 50% were considered. All columns had the same D/t ratio of 50, and L/D ratio of 4. The compressive strength of concrete core and the yield stress of steel tube were 22.5 MPa and 240 MPa, respectively. The stress-strain relation for the steel tube was considered as bilinear with a strain

hardening slope at 1% of the initial elastic modulus of steel.

The maximum lateral strength of CFT columns (depicted at Table 4) are evaluated with analytical model and code's provisions vs. N/N_0 ratio (axial load level) is shown in Fig. 10. The Fig.11 shows the ratios of code values to values predicted by present study for changing N/N_0 . With comparison of these curves, some conclusions can be expressed:

i. During the increasing of axial loads the predicted strength of two codes are far from each other. For each level of axial loads, AISC-LRFD values always are conservative. For high range of axial loads ($N/N_0=0.5$), ACI shows no conservative strength. It alludes to high local buckling in the steel shell that

Table 4. Properties of specimens for the axial load level case study

Specimen No.	Section	N (kN)	N/N_0	D (mm)	t (mm)	L (mm)	L/D	D/t	f'_c (MPa)	f_y (MPa)	E_s/E_s
SC-N-I	Square	0	0.00	300	6	1200	4	50	22.5	240	0.01
SC-N-II		557	0.20	300	6	1200	4	50	22.5	240	0.01
SC-N-III		976	0.35	300	6	1200	4	50	22.5	240	0.01
SC-N-IV		1394	0.50	300	6	1200	4	50	22.5	240	0.01
CC-N-I	Circle	0	0.00	300	6	1200	4	50	22.5	240	0.01
CC-N-II		444	0.20	300	6	1200	4	50	22.5	240	0.01
CC-N-III		777	0.35	300	6	1200	4	50	22.5	240	0.01
CC-N-IV		1110	0.50	300	6	1200	4	50	22.5	240	0.01

$$EI = (E_c I_c / 5) / (1 + \beta_d) + E_s I_s \quad (2)$$

$$P_0 = A_s f_y + 0.85 A_c f'_c \quad (3)$$

$$t_{min} = 0.58 b \sqrt{f_y} \text{ (ACI)} , \quad t_{min} = 0.44 b \sqrt{f_y} \text{ (AISC - LRFD)} \quad \text{Square Sections} \quad (4a)$$

Fig. 10. The lateral strength of columns vs. axial load level aspect ratio

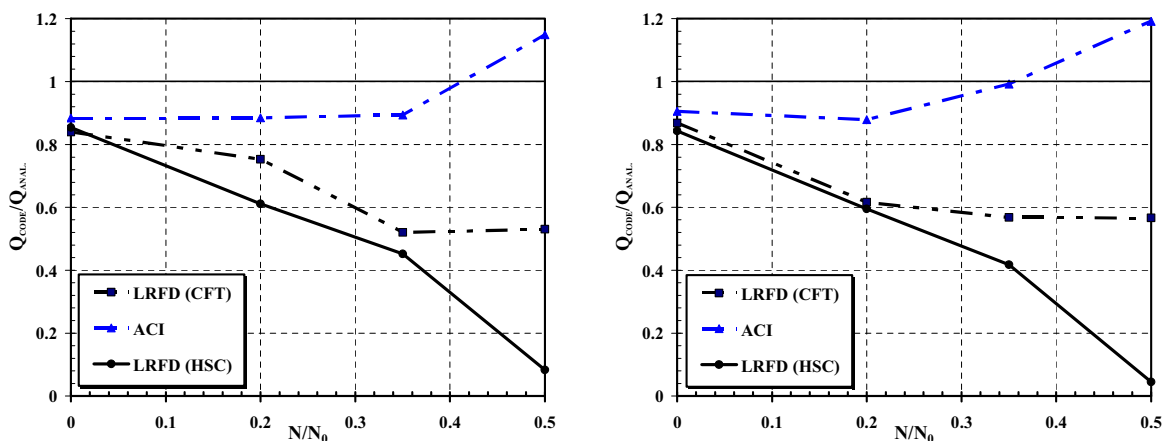


Fig. 11. The comparison between codes and present study for changing axial load level

is not contemplated in ACI codes.

ii. The analytical strength shows an increasing of strength in first stage of increasing of axial load ($N/N_0=0.2$) after that, the strength reduced with increasing of axial load. ACI shows similar variations but AISC-LRFD doesn't show this variations. In this code the strength reduce with increasing axial load during increasing axial loads.

iii. Without axial load, the two codes supply the lower strength for CFT column than analytical strength respect to hollow section.

iv. The lateral strength's estimations of AISC-LRFD for CFT columns are lower than analytical result of hollow sections.

v. ACI shows more superior estimations of lateral strength to AISC-LRFD.

vi. With increasing axial load AISC-LRFD shows more declining of shear strength to ACI.

7. Conclusions

A 3-D finite element model was developed to compare accuracy of codes in evaluation flexural strength of CFT and HSC columns under a constant axial load, for a number of different geometric and material parameters. The following conclusions may be drawn:

1. The minimum thickness that recommended in preventing local buckling before steel shell yielding by - mentioned codes, for CFT columns could be decreased up to %30 especially for square section based on ACI code.

2. In estimation of lateral strength of CFT columns the ACI is reasonable than AISC-LRFD.

3. The measured shear capacity by ACI generally higher than their counterparts computed by AISC-LRFD.

4. AISC-LRFD estimates the lateral strength conservatively but ACI in some ranges such as in short columns and in high axial load levels computes lateral strength in no conservative manner.

5. The effects of some parameters, such as local buckling in column with high aspect ratio and shear deformation in column with low slenderness and high level of axial load that could influence CFT response seriously, should be taken in to account in the design process.

References

- [1] Building Code Requirements for Structural Concrete and Commentary: 2008, ACI 318-08, Am. Concrete Inst., Detroit, Mich.
- [2] Specification for Structural Steel Buildings: 2005, ANSI/AISC 360-05.
- [3] Euro code 4: 2004, ENV 1994-1-1, Design of composite steel and concrete structures, Part 1.1, General rules and rules for building, Commission of European Communities.
- [4] CSA: 2007, Limit States Design of Steel Structures - CAN/CSA-S16-01, Canadian Standards Association, Rexdale, Ontario, Canada, 700p.
- [5] CECS 28:90: 1991, Specification for the Design and Construction of Concrete-Filled Steel Tubular Structures, China Planning Press, Beijing, (in Chinese)
- [6] Architectural Institute of Japan: 1997, AIJ, Recommendations for design and construction of concrete filled steel tubular structures, Tokyo.
- [7] Furlong, R. W.: 1967, Strength of Steel-Encased Concrete Beam-Columns, J. of Struct. Div., ASCE, Vol. 93, No. ST5, pp. 267-281.
- [8] Furlong, R. W.: 1968, Design of Steel-Encased Concrete Beam-Columns, J. of Struct. Div., ASCE, Vol. 94, No. ST1, pp.267-281.
- [9] Gardner, J., and Jacobson, R.: 1967, Structural Behavior of Concrete Filled Steel Tubes, ACI Journal, Vol. 64, pp. 404-413.
- [10] Park, R. J. T., Priestley, M. J. N., and Walpole W. R.: 1983, Reinforced concrete bridge piles, Bulletin of the New Zealand National Society for Earthquake Engineering 16.
- [11] Liu, Z., Goel, C.: 1988, Cyclic load behavior of concrete-filled tubular braces, J. Struct. Eng. ASCE, 114.
- [12] Abdel Salam, M. N., Abdel Ghaffar, M., and Zaki, M. A.: 2001, Axial load capacity of short circular concrete filled steel tubes - An analytical model, Journal of Engineering and Applied Science, 48, 473-490.
- [13] Sakino, K., Nakahara, H., Morino, S, and Nishiyama, I.: 2004, Behavior of Centrally Loaded Concrete-Filled Steel-Tube Short Columns, J. Struct. Eng. ASCE, 124, 180-188.
- [14] Sakino, K., Tomii, M.: 1981, Hysteretic behavior of concrete filled square shell tubular beam-columns failed in flexure, Transaction of the Japan Concrete Institute (Tokyo) 3, 439-446.
- [15] Sakino, K., Ishibashi, H.: 1985, Experimental studies on concrete filled square steel tubular short columns subjected to cyclic shearing force and constant axial force, Transactions of the Architectural Institute of Japan (Tokyo) 353, 81-89.
- [16] Tomii, M., Sakino, K., Xiao, Y., and Watanabe, K.: 1985, Earthquake resisting hysteretic behavior of reinforced concrete short columns confined by steel tube experimental results of preliminary research, Proc. of the International Specialty Conference on Concrete Filled Steel Tubular Structures, Harbin, China, 119-125.
- [17] Sugano, S., Nagashima, T.: 1992, Seismic behavior of concrete filled steel column." Proc. Tenth Structural Congress ASCE, 914-917.
- [18] Morino, S., Kaawaguchi, J., Yasuzaki, C., and Kanazawa, S.: 1992, Behavior of concrete filled steel tubular three dimensional sub-assemblages, Proc. Composite Construction in Steel and Concrete II ASCE, 726-741.
- [19] Usami, T., Ge, H.: 1994, Ductility of concrete-filled steel box columns under cyclic loading, J. Struct. Eng. 120, 2021-2039.
- [20] Boyd, P. F., Cofer W. F., and Mclean D. I.: 1995, Seismic performance of steel encased concrete columns under flexural loading, Struct. J. ACI 92, 355-364.
- [21] Ge, H., Usami, T.: 1996, Cyclic tests of Concrete-Filled Steel box columns, J. Struct. Eng. ASCE, 122, 1169-1177.
- [22] Ge, H., Usami, T.: 1994, Strength analysis of concrete-filled thin-walled steel box column, J. Constr. Steel Res. 30, 259-281.
- [23] Uy, B.: 2000, Strength of concrete filled steel box columns incorporating local buckling, J. Struct. Eng. ASCE, 126, 341-352.
- [24] Tomii M., and Sakino K.: 1979, Elasto-plastic behavior of concrete filled square steel tubular beam-column, Trans. Arch. Inst. Of Japan, Japan, 280, pp. 111-120.
- [25] Wakabayashi, M., Minami, K.: 1981, Rational analysis of shear in structural concrete columns, Disaster Prevention Research Institute Annuals, Kyoto University, 24 B-1.
- [26] Hajjar, J. F., Gourley, B. C.: 1996, Representation of concrete-filled steel tube cross-section strength, J. Struct. Eng. ASCE 122, 1327-1336.
- [27] Hatzigeorgiou G.D.: 2008, Numerical model for the behavior and capacity of circular CFT columns. Part I: Theory, Engineering Structures; 30(6): 1573-1578.
- [28] Hatzigeorgiou G.D.: 2008, Numerical model for the behavior and capacity of circular CFT columns. Part II: Verification and extension, Engineering Structures; 30 (6) 1579-1589.
- [29] Shams, M., Saadeghvaziri, M. A.: 1999, Nonlinear response of CFT columns under axial load, Struct. J. ACI, 96, 1009-1017.
- [30] Hajjar, J. F., Gourley, B. C.: 1997, A cyclic nonlinear model for concrete-filled tubes I: Formulation & II: Verification, J. Struct. Eng. ASCE 123.

- [31] Hajjar, J. F., Schiller, P. H., Molodan, A.: 1998, A distributed plasticity model for concrete-filled steel tube beam-columns and composite frames, *Eng. Struct.* ACSE 20, 398-412.
- [32] Hajjar, J. F., Molodan, A., Schiller, P. H.: 1998, A distributed plasticity model for cyclic analysis of concrete-filled steel tube beam-columns with interlayer slip, *J. Eng. Struct.* ASCE 20, 663-676.
- [33] Golafshani, A. A., Aval, B. B., Saadeghvaziri, M. A.: 2001, An Efficient Fiber Element for Cyclic Analysis of CFT Columns, *Asian Journal*, Vol. 1, No. 3.
- [34] Aval, S. B. B., Saadeghvaziri, M. A., Golaafshani, A. A.: 2002, A comprehensive composite inelastic fiber element for cyclic analysis of CFT columns, *J. Eng. Mech.* ASCE 128, 428-437.
- [35] Lundberg, J. E.: 1993, The reliability of composites and beam columns, *Struct. Engrg. Rep. No. 93-2*, Dept. of Civ. And Mineral Engrg., Univ. of Minnesota, Minneapolis.
- [36] Schneider, S. P.: 1998, Axially loaded concrete-filled steel tubes, *J. Struct. Eng.* ASCE, 124, 1125-1138.
- [37] Zhang, W., Shahrooz, B.: 1999, Comparison between ACI and AISC for concrete-filled tubular columns, *J. Struct. Eng.* ASCE, 125, 1213-1223.
- [38] Lue, D.M., Liu, J., Yen, T.: 2007, Experimental study on rectangular CFT columns with high-strength concrete, *J. of Const. St. Res.* 63, 37-44
- [39] AS 5100.6: 2004, Bridge design Part 6: Steel and composite construction, Sydney (Australia): Australia Standards; 2004.
- [40] ANSYS®: 2008, Structural nonlinearities manual, SAS IP Inc.
- [41] Willam, K. J., Warnke, E. D.: 1975, Constitutive model for the triaxial behavior of concrete, *Proc. International Association for Bridge and structural Engineering*, Ismes, Bergamo, Italy, 19, 174.
- [42] Nakai, H., Kurita, L., Ichinose, H.: 1991, An experimental study on creep of concrete filled steel pipes, *Proc. 3rd Int. Conf. Steel-Concrete Compos. Struct.*, M. Wakabayashi, ed., Assn. For Int. Cooperation and Res. In steel-Concrete Compos. Struct., 55-65.
- [43] Eggert, G. M., Dawson, P. R., Mathur, K. K.: 1991, An adaptive descent method for nonlinear viscoplasticity, *Int. J. Numer. Methods Eng.* 31, 1031-1054.
- [44] Crisfield, M. A.: 1982, Local instabilities in the non-linear analysis of reinforced concrete beams and slabs, *Proc. Instn. Civ. Engrs.*, PT 2, 73, 135-145.
- [45] Crisfield, M. A.: 1986, Snap-through and snap-back response in concrete structures and the dangers of under-integration, *Int. J. Numer. Methods Eng.* 22, 751-767.
- [46] Golafshani, A. A., Aval, S. B. B., Saadeghvaziri, M.,A.: 2002, The fiber element technique for analysis of concrete- filled steel tubes under cyclic loads, *Struct. Eng. and Mech.*, Vol. 14, No. 2, August, pp. 119-133.

List of symbols

- A_c section area of concrete
- A_s area of steel section
- b overall width of rectangular CFT section.
- β_d the ratio of the maximum factored axial sustained load to the maximum factored axial load.
- CFT* concrete filled steel tubes
- D overall width of circular CFT section.
- E_c elastic modulus of concrete
- E_s elastic modulus of steel
- E'_s strain hardening slope of steel
- f_y or σ_y yield strength of steel
- f'_y specified compressive strength of concrete core.
- HSC* hollow steel column
- I_c moment of inertia of section for concrete
- I_s moment of inertia of section for steel
- P_c elastic load buckling
- K load buckling coefficient
- L is column length.
- N applied axial load.
- N_0 axial load column capacity
- P_u The design axial load strength
- P_n The nominal axial load strength
- R drift ratio
- t thickness of steel jacket
- t_{min} minimum thickness of steel jacket based on codes provisions